ORIGINAL ARTICLE

Parameter Optimization for Cost Reduction of Microbubble Generation by Electrolysis

Arpon Lucero Jr, Dong-Seog Kim, Young-Seek Park[1]*

Department of Environmental Science, Catholic University of Daegu, Gyeongsan 38430, Korea
[1]DU University College, Daegu University, Gyeongsan 38453, Korea

Abstract

To lower the operational cost of microbubble generation by electrolysis, optimization of parameters limiting the process must be carried out for the process to be fully adopted in environmental and industrial settings. In this study, four test electrodes were used namely aluminum, iron, stainless steel, and Dimensionally Sable Anode (DSA). We identified the effects and optimized each operational parameter including NaCl concentration, current density, pH, and electrode distance to reduce the operational cost of microbubble generation. The experimental results showed that was directly related to the rate and cost of microbubble generation. Adding NaCl and narrowing the distance between electrodes caused no substantial changes to the generation rate but greatly decreased the power requirement of the process, thus reducing operational cost. Moreover, comparison among the four electrodes operating under optimum conditions revealed that aluminum was the most efficient electrode in terms of generation rate and operational cost. This study therefore presents significant data on performing cost-efficient microbubble generation, which can be used in various environmental and industrial applications.

Key words : Operational cost, Microbubble generation rate, pH, Electrode distance, NaCl concentration

1. Introduction

In recent years, generation of microbubbles has received quite an attention for many researchers due to its favorable outcome in solid-liquid separation and purification. Microbubbles have been used primarily for the treatment of water and wastewater (e.g. air floatation, oxygen supplying) however, its application has currently reached food, bioprocessing, energy industries and now even being applied in medical fields (Nagai et al., 2003; Weber and Agblevor, 2005; Araya-Farias et al., 2008; Tan et al., 2016). In general,

there are number of ways of generating microbubbles but conventional flotation methods like Dissolved Air Flotation (DAF), Induced Air Flotation (IAF), and Electroflotation (EF) are more commonly used (Rubio et al., 2002).

Dissolved Air Flotation (DAF) is a microbubble generation method that has been utilized to treat water and wastewater. In this method, air is dissolved under pressure (3 ~ 4 atm) into the solution and then released through decompression needle valves to atmospheric pressure which causes the formation of microbubbles (Parmar and Majumder, 2013). DAF has been

effective in separating fine particles due to its relatively small and uniform microbubbles. However, the overall process efficiency is reduced due to some disadvantages like high energy requirement, complex system and expensive service cost (Li, 2006). Induced Air Flotation (IAF) is an alternative method to DAF in wastewater treatment. IAF generates air bubbles through the use of mechanical agitation or gas sparger which is usually simple and cost effective (Bloom and Heindel, 2003; Li, 2006). The only disadvantage of IAF is that it generates larger bubbles three times the size of bubbles generated by DAF. The larger the bubbles generated, the lower the bubble - particle collision and attachment efficiencies (Lee and Lee, 2002; Li and Tsuge, 2006) which results to poor efficiency especially in solid-liquid separation processes. Electroflotation (EF) is another method of microbubble generation based on the principles of electrolysis which is now commonly used in a wide range of industrial applications (Nagai et al., 2003; Araya-Farias et al., 2008; Bande et al., 2008; Rahmani et al., 2013; Baierle et al., 2015; Mota et al., 2015). In this method, by allowing a current flow through the electrodes, water undergo redox reactions splitting water into H_2 and O_2 in the form of microbubbles at the cathode and anode, respectively (Burns et al., 1997). Similar to DAF, it is also a very effective process (Rahmani et al., 2013; Baierle et al., 2015; Mota et al., 2015). Among the three methods discussed, EF generates the smallest and most uniform microbubbles making it the preferred method to use in this study (Burns et al., 1997; Araya-Farias et al., 2008).

In flotation, rate of microbubble generation in homogeneity is one of the key elements for efficient process. According to Bennett et al.(1958), flotation rate can be increased not only by reducing the bubble size but also by generating more bubbles. Higher bubble flux provides more opportunities for collisions. Many of the earlier studies on microbubble generation

by EF were focused on bubble size distributions (Khosla and Venkatachalam, 1991; Mansour et al., 2007; Luiyi et al., 2014; Chandran et al., 2015) which provides information only on the frequency of microbubbles generated with respect to their sizes. Limited data are available on the actual rate of microbubble generation (Burns et al., 1997) which, apparently, one of the key aspects to an efficient process. Theoretically, the rate of microbubble generation can be computed (Chen and Chen, 2010) but theoretical values are only used to predict an outcome in an ideal environment and not in real condition where inhibiting factors exist.

The aim of this study is to introduce a straight forward and simpler approach in quantifying the actual rate of microbubble production using electrolysis method. Moreover, evaluate the effects of main operating parameters such as sodium chloride (NaCl) concentration, current density, pH and electrode distance on the rate of microbubble generation and power consumption and finally, optimize these operating parameters based on microbubble generation cost of four different electrode materials.

2. Experimental

2.1. Electrode materials

Two different types of electrodes (Sacrificial and non-soluble type of electrodes) were used in this experiment. Sacrificial electrodes consisted of aluminum (Al), and iron (Fe) while non-soluble electrodes included stainless steel (Sus) and Dimensionally Sable Anode (DSA). Aluminum, iron and stainless steel plates were purchased locally all with the same thickness. They were cut into square sheets with an area of 12.25 cm^2 (3.5 cm x 3.5 cm) and an excess of about 0.5 cm^2 for the wire connection. DSA was made by coating Ru-Ir-Ti mixture on the surface of the Titanium (Ti) plate. Coating was made by brushing Ru-Ir-Ti mixture onto the surface until the
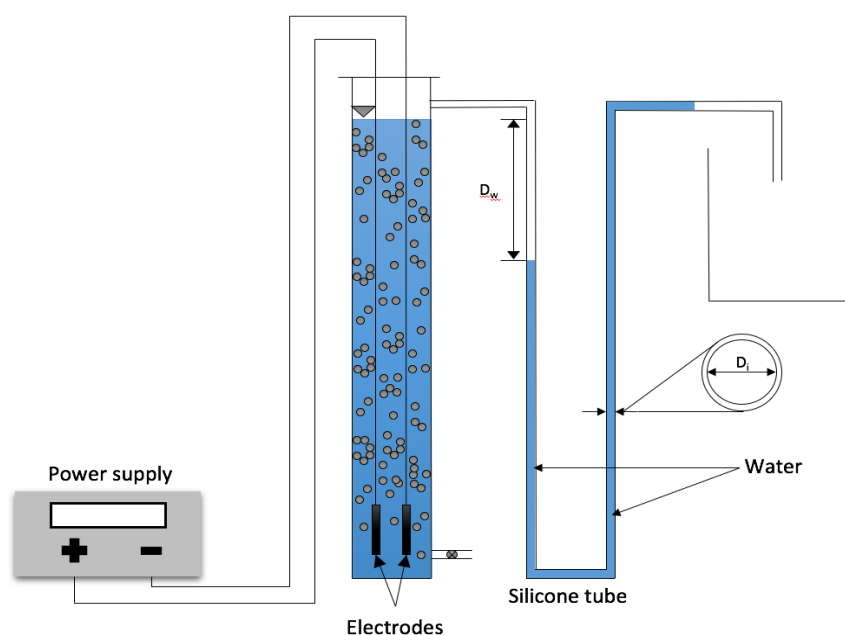
Fig. 1. Schematic diagram of bubble volume measuring device.

metal exterior was completely covered. The electrode was then dried in a muffle furnace (model DMF802, Daeil Engineering co., LTD) at 450ºC for 60 minutes and let it cool down at room temperature before the start of the second coating. Subsequent coating and drying were done 10 times to make the DSA electrode.

2.2. Experimental Set-up

Fig. 1 shows the schematic diagram of the microbubble volume measuring device. This experimental set-up was adopted from a previous work (Park, 2006) which, consisted of a chamber, pair of electrodes, a silicon tube and a DC power supply. Two chambers with total volume of 450 cm^3 and 1,008 cm^3 were fabricated and the chamber with larger volume was used for the electrode distance experiment. The port at the top portion of the chamber was mounted with silicon tube (9 mm diameter) where generated gas bubbles travelled through. Every electrode pair was fixed by an electrode holder exposing a total of 10.5 cm^2 effective surface area and

was placed vertically at the bottom of the chamber with an initial distance of 6 mm between each electrode. Finally, an external DC power supply (GW GPR-11H30D) was connected to the opposite end of the wire which served as the source of power for the entire experiment. To ensure accurate readings, the set up was checked for leakages by running water in and out of the chamber before and in between experiments.

Deionized water was used as the test liquid and then mixed with NaCl before pumping the solution inside the chamber through the lower port using a cartridge pump (masterflex L/S model 7518-10). The pH of every salt solution used was initially adjusted using a pH meter (Suntex SP2300) and 0.1 and 1.0 mole of NaOH and HCl solutions. For a steady gas flow, newly formed microbubbles were first allowed to partially fill up the chamber for 1 minute before the displaced liquid inside the silicon tube is measured so that more precise results are obtained. The

measurements were done every minute for seven minutes. The voltage was recorded at the end of each run for computation purposes. The rate of microbubble generation was then determined by calculating the average volume of the displaced liquid in every minute of electrolysis.

2.3. Microbubble generation analyses

The average microbubble generation rate was determined by measuring the displacement of the water inside the silicon tube every minute for seven minutes and then, the average water displacement was computed. The average microbubble generation rate (AGR) was then calculated by multiplying the average water displacement with the cross-sectional area of the silicon tube. This can be represented by the equation:

$$AGR = D_w \times (\pi D_i^2/4) \tag{1}$$

where, AGR is the average generation rate (cm^3/min), D_w is the average water displacement rate (cm/min) and D_i is the inside diameter of the silicon tube (Fig. 1).

NaCl concentration, current density, pH and electrode distance were evaluated using a one-parameter-at-a-time approach where optimum values were determined based on the lowest cost of 1,000 L of microbubbles generated. The system was assumed to be a multi-cell electrolysis process in which the number of cells is highly dependent on the duration of the operation. It should be noted that only the operational costs (NaCl and power) were included in the computations. Other possible costs such as the purchase of electrode, reactor construction, and pH adjustments were not included. Local industrial prices of NaCl and power were identified to be 0.88 USD per kilogram and 0.052 USD per kWh, respectively, and these amounts were the ones used in the computations. One optimum value was selected after each parameter or experiment set. Subsequent experiments were then performed using the previously selected optimum value until all experiments were completely executed.
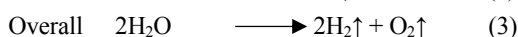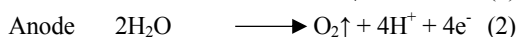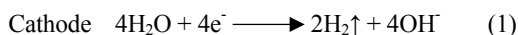
3. Results and Discussion

Every set of experiments was performed to evaluate the effect of NaCl concentration, current density, pH and electrode distance on the rate of microbubble generation with different electrode materials and to optimize each of these operating parameters to reduce the operational cost.

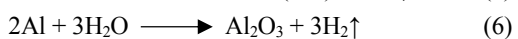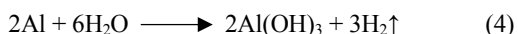### 3.1. Effect of NaCl concentration

Fig. 2(a) shows the average volume of bubbles generated per minute at varied NaCl concentrations between 0.1 to 10 g/L while keeping other parameters constant. Results indicate different microbubble generation rates according to type of electrode showing two trends which conforms to previous studies utilizing different electrode type (Jansenn et al., 1983; Burns et al., 1997; Park, 2006): (1) the rate of microbubble generation of non-soluble electrodes slightly decrease at higher NaCl concentration (2) the rate of microbubble generation of sacrificial electrodes slightly increase at higher NaCl concentration. Although this change is noticeable on the graph, it is so small that it can be considered an insignificant variation on microbubble generation. However, it is clearly obvious that aluminum exhibits the highest rate of microbubble generation when considering electrode type. The plausible reason behind the high microbubble generation rate of aluminum is the reaction that happens between aluminum and water. Aside from the splitting of water molecule into H_2 and O_2 during electrolysis (1, 2), aluminum also reacts with water molecule to form aluminum hydroxide complexes and hydrogen gas (Petrovic and Thomas, 2008). Electrolysis can be described by the reactions below:
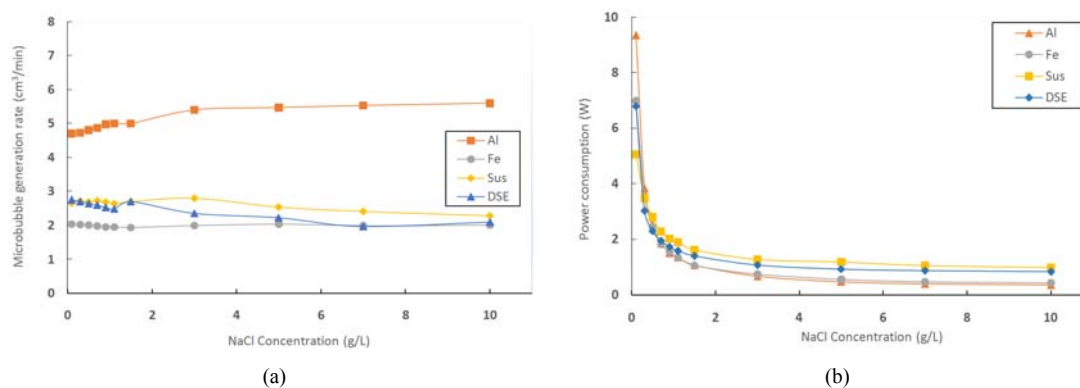
Fig. 2. Effect of NaCl concentration on (a) rate of microbubble generation and (b) power consumption
(Current density = 23.81 mA/cm^2; pH = 7; Electrode distance = 6 mm).

Cathode $4H_2O + 4e^- \longrightarrow 2H_2\uparrow + 4OH^-$ (1)

Anode $2H_2O \longrightarrow O_2\uparrow + 4H^+ + 4e^-$ (2)

Overall $2H_2O \longrightarrow 2H_2\uparrow + O_2\uparrow$ (3)

Possible reactions of aluminum with water are the following:

$2Al + 6H_2O \longrightarrow 2Al(OH)_3 + 3H_2\uparrow$ (4)

$2Al + 4H_2O \longrightarrow 2AlO(OH) + 3H_2\uparrow$ (5)

$2Al + 3H_2O \longrightarrow Al_2O_3 + 3H_2\uparrow$ (6)

Reactions 4, 5, and 6 promote further generation of hydrogen gas which could explain the higher bubble generation rate in aluminum compared to the rest of the electrodes based on the results.

Unlike its minor effect on microbubble generation, NaCl concentration has an immense impact on power. When NaCl is added to water, it ionizes, affecting the electrical conductivity of the solution such that when a number of ions further increase, transport of electrons to and within the solution becomes much easier (Opu, 2015). This occurrence decreases the total voltage within the system thereby reducing power consumption. As shown in Fig. 2(b), there is a rapid decrease in power consumption from 0 to 2 g/L of NaCl. This sudden decrease is because of the presence of more

ionic substances in the solution which apparently makes the travel of electrons much easier lowering voltage and power consumption accordingly.

3.2. Effect of current density

Current density is critical to an electrolysis process because it serves as the key player in achieving higher bubble flux that provides more opportunity for collision as a result (Bennet et al., 1958). Increasing the current is basically increasing the flow of electrons into the circuit which accelerates the rate of nucleation. According to Faraday's law of electrolysis, the mass of substance altered at an electrode's surface during electrolysis which, in this case water, is directly proportional to the quantity of electricity transferred to that electrode (Opu, 2015) thus, evolution of hydrogen and oxygen bubbles on the electrode's surface increases with the increase of the applied current. Moreover, increasing the current also increases the active nucleation sites where evolution of more microbubbles takes place (Alam, 2015).

Similar to the effect of NaCl concentration, each electrode shows differences in generation rates at varying current densities. Fig. 3(a) shows that at 4.76 mA/cm^2, iron, stainless steel and DSA electrodes are almost equal. As current density increases, rate of

(a)   (b)
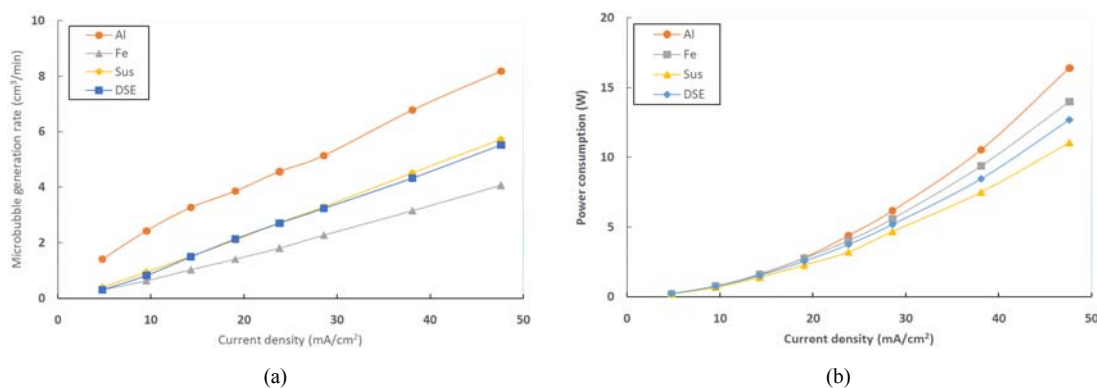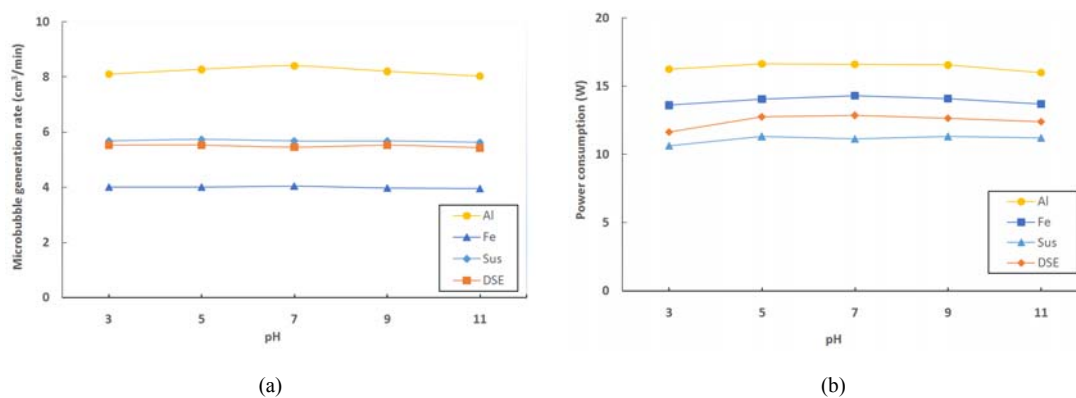
Fig. 3. Effect of current density on (a) rate of microbubble generation and (b) power consumption
(NaCl concentration = 0.30 g/L; pH = 7; Electrode distance = 6 mm).

bubble generation also increases. However, iron generates bubbles much slower than stainless steel and DSA making it the lowest in terms of microbubble generation. The reason why iron has a very poor generation rate might be due to the oxygen not forming at the anode rather, the iron oxide present are dehydrated iron hydroxides (Moreno et al., 2007).

At 47.62 mA/cm^2, 5.73 cm^3 and 5.52 cm^3 of microbubbles per minute are generated with stainless steel and DSA electrodes, respectively. That is 15 and 19 times faster microbubble generation rate compared to the case at 4.76 mA/cm^2. Moreover, at same current density, microbubble generation rate of aluminum is 8.18 cm^3/min, 6 times higher compared to the generation rate of 1.41 cm^3/min at 4.76 mA/cm^2 and will further increase at higher current densities based on the trend. It is important to note however, that increasing the applied current also increases the power consumption that is consumed by the process thus increase in operational cost (Fig. 3(b)). Differences in power consumption among all electrode types are noticeable beyond 19.05 mA/cm^2. In theory, power consumption is equal to the applied current multiplied by the total cell voltage which is a contribution of different types of overpotential namely activation, concentration, ohmic and the cell's reversible

potential (Alam, 2015). The reason for the differences in power of each electrode in higher current density can be explained mainly by these overpotentials on both electrodes. When water is electrolyzed, it undergoes redox reactions splitting H_2O into H_2 and O_2 (3). Reduction of hydrogen happens at the cathode when water molecule gains electrons forming $H_{2(g)}$ and $OH^-_{(aq)}$ (1). The $OH^-_{(aq)}$ accumulates around the cathode making the region more negative. Likewise, when water molecule loses electron at the anode, O_2 and H^+ are produced (2). Over time, H^+ accumulation around the anode makes the region more positive. This difference in the concentration of ions between electrodes makes the voltage really high as accumulated ions adjacent to the surface of the electrodes produce a concentration gradient which causes diffusion of current (Alam, 2015). Moreover, if sacrificial electrodes (e.g. aluminum and iron) are used, increased in applied current also increases the oxidation rate of the anode (dissolution) forming resultant cations (Al^{3+}, Fe^{2+}). These cations are liberated near the anode which makes the region even more positive. It is therefore understandable why aluminum and iron have higher power requirement (Fig. 3(b)) over the other electrodes which do not dissolve or just partially dissolved.

(a)   (b)

Fig. 4. Effect of pH on (a) rate of microbubble generation and (b) power consumption
(NaCl Concentration = 0.3 g/L; Current density = 47.62 mA/cm^2; Electrode distance = 6 mm).

3.3. Effect of pH

Many previous researchers have reported pH as one of the main parameters that affects many electrolysis based processes especially electrocoagulation and electroflotation (Adhoum et al., 2004; Gao et al., 2009; Keshmirizadeh et al., 2011). There are no available reports which, directly relates pH to the actual rate of microbubble generation. However, a related study was recently conducted by Goor(2015) about the influence of temperature and pH on hydrogen evolution reaction on platinum. He reported that the overall reaction rate increased based on increasing exchange current density at higher pH thus indicates that microbubble generation is faster at higher pH values.

To address this information gap, we conducted series of experiments that would determine the effect of pH on the actual microbubble generation rate using various electrode materials and found out that pH has no influence on microbubble generation (Fig. 4(a)). Moreover, the addition of diluted NaOH and HCl to adjust the pH of the solution might have partially increased the presence of ions but not sufficient to actually have a positive effect on power consumption (Fig. 4(b)).

3.4. Effect of electrode distance

As expected, there were no significant changes on the rate of microbubble generation at different electrode distances (Fig. 5(a)). Again, according to Faraday's law of electrolysis, the mass of substance altered at an electrodes surface is directly proportional to the quantity of electricity transferred to that electrode (Opu, 2015). In other words, the current which represents the flow of electrons dictates the generation of gas bubbles on electrodes surface. Narrowing the space between the electrodes will decrease the cell voltage (Nagai et al., 2003; Opu, 2015) but not the current which has the direct control of the generation rate. In terms of power consumption, however, significant changes are observed. Fig. 5(b) illustrates the relationship between electrode distance and power consumption. At the largest electrode distance of 15 mm, all four electrodes showed the highest energy requirement and as the distance between electrodes becomes narrower, the energy requirement also decreases. The results obtained in this investigation agrees with the result of some previous studies (Nagai et al., 2003; Opu, 2015) who reported a lower cell voltage at shorter electrode distance as electrons require lesser energy to move across the electrolyte bulk.

| (a) | (b) |
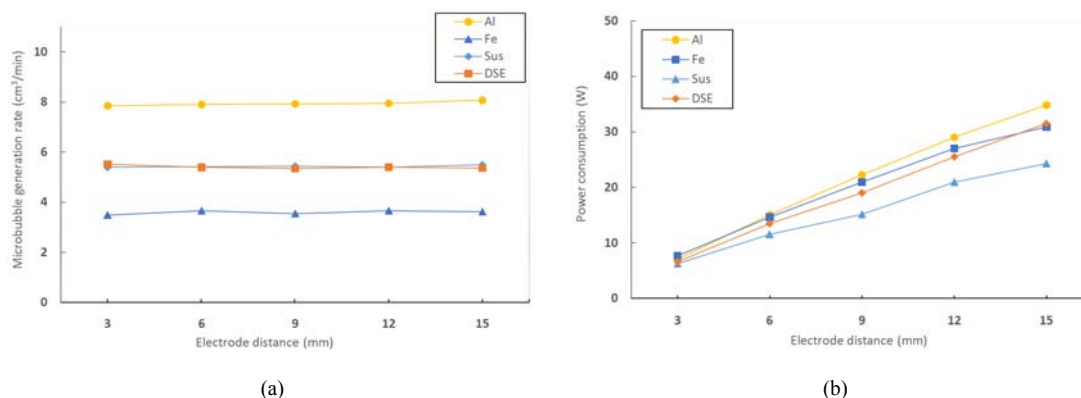
Fig. 5. Effect of electrode distance on (a) rate of microbubble generation and (b) power consumption
(NaCl concentration = 0.3 g/L; Current density = 47.62 mA/cm^2; pH = 7).

3.5. Selection of optimum parameters

In this section, determination of the optimal NaCl concentration, current density, pH and electrode distance is discussed. As stated previously, one of the main purpose of this study is to determine the optimum operating parameters based on the microbubble generation cost. It is important to note however that only the operational costs (NaCl, power) were included in the computations and was based on every 1,000 liters of microbubbles generated assuming the process is running in multiple reactor units. Other possible constructional costs such as the purchase of electrode, reactor construction and pH adjustments were not included.

Fig. 6(a) shows the total operational cost of microbubble generation at varying NaCl concentration. The graph shows that NaCl range of 0.3 ~ 0.5 g/L has the lowest generation cost of 1,000 L of microbubbles in all electrodes. Beyond 0.5 g/L of NaCl, the power reduction becomes insignificant while NaCl cost started to increase tremendously. So for the optimum NaCl concentration, we selected 0.3 g/L since it is the cheapest for all electrodes. Table 1 shows the operational cost breakdown of all four electrodes at different NaCl concentration.
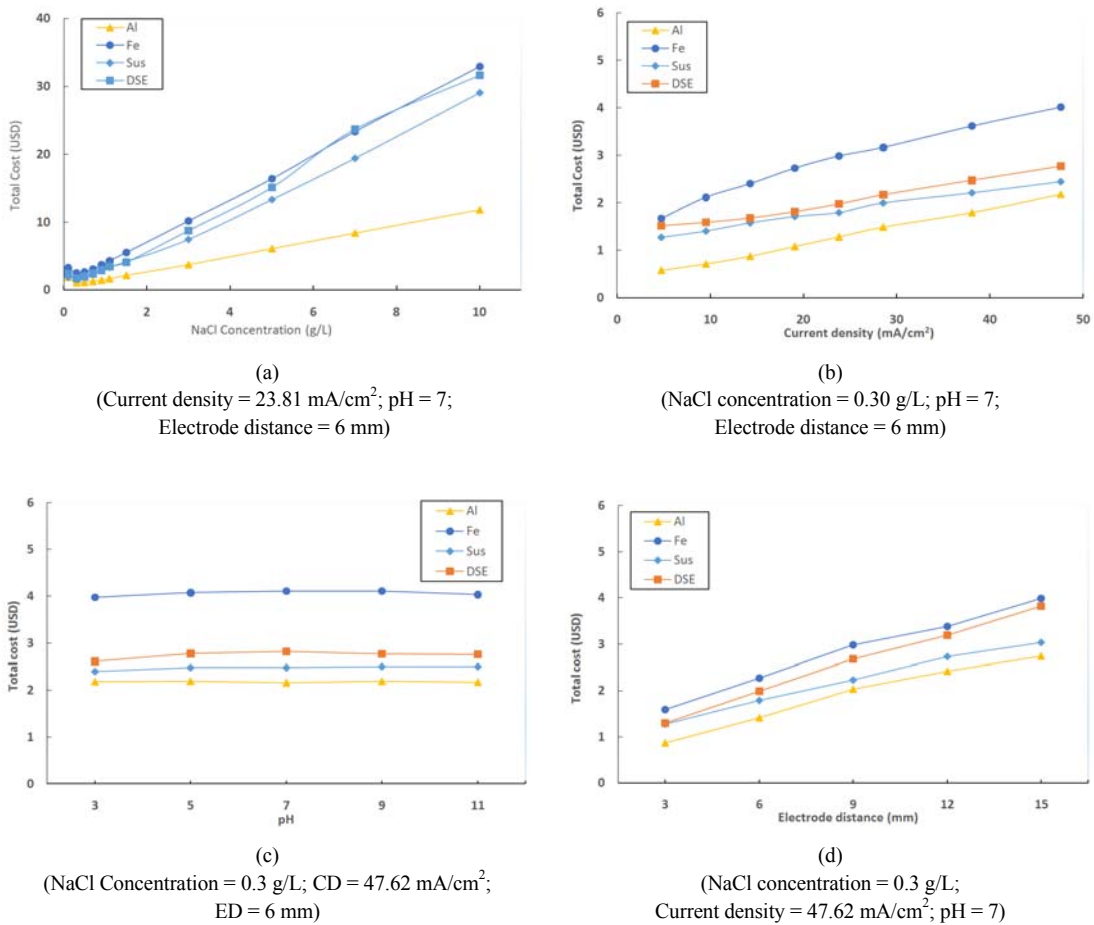
Fig. 6(b) shows the total cost at varying current density. The graph illustrates that operational cost also increases as current density increases. Although it is apparent that 4.76 mA/cm^2 current density is the cheapest, we decided to select the highest current density which is 47.62 mA/cm^2 as our optimum for the reason that at higher current densities, generation rate is faster. At 47.62 mA/cm^2 for example, generation of 1,000 L of microbubbles assuming 100 reactor units are used would only take 21 hours while 4.76 mA/cm^2 would take 119 hours of continued electrolysis. This is the reason why we have chosen the highest current density as our optimum.

For the optimum pH value, it has been discussed that pH has no effect on power thus in operational cost as well. That is evident on Fig. 6(c) where the cost at varying pH are almost the same in each electrode. Hence, we selected pH 7 as our optimum for the reason that pH 7 is the natural condition. In application, however, it is recommended to maintain the original initial pH to avoid additional cost due to pH adjustments especially when considering large scale process.

Finally, for electrode distance shown in Fig. 6(d), 3 mm electrode distance exhibited the cheapest cost of generation therefore it was selected as the optimum.

(a)
(Current density = 23.81 mA/cm^2; pH = 7;
Electrode distance = 6 mm)

(b)
(NaCl concentration = 0.30 g/L; pH = 7;
Electrode distance = 6 mm)

(c)
(NaCl Concentration = 0.3 g/L; CD = 47.62 mA/cm^2;
ED = 6 mm)

(d)
(NaCl concentration = 0.3 g/L;
Current density = 47.62 mA/cm^2; pH = 7)

Fig. 6. Operational cost of all four electrodes at (a) varying NaCl concentration, (b) varying current density, (c) pH and (d) different electrode distance.

3.6. Comparison among electrode materials

Using all optimum parameters, we are able to compare the efficiency of each electrode based on the rate of microbubble generation, power consumption and operational cost. Fig. 7 shows the optimized results. Among the four electrodes, the iron has the lowest microbubble generation rate and it has the highest power requirement and thus have the most expensive cost for generating 1000 L of microbubbles. Possible reason for such high cost is the formation of rust layers on the surface of iron electrode. Rust inhibits the flow of current increasing the overall resistance which increases the power requirement and lead to higher operating cost.

Non-soluble electrode such as stainless steel and DSA are almost the same in terms of generation rate. However, based on the results, stainless steel electrode generates a little less microbubble but also requires less power than DSA. So, even though there is a disparity on the rate of microbubble generation between the non-soluble electrodes (stainless steel and DSA), their total operating cost are practically the same. They generate microbubbles at an average rate with a relatively low power requirement as compared
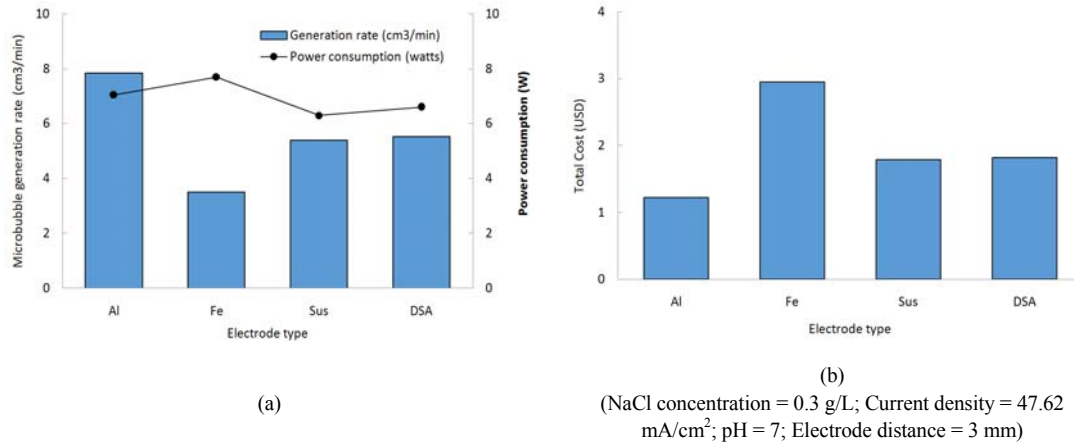
(a)

(b)

(NaCl concentration = 0.3 g/L; Current density = 47.62 mA/cm^2; pH = 7; Electrode distance = 3 mm)

Fig. 7. Optimized (a) generation rate, power and (b) overall cost of all four electrodes.

the rest of the electrodes.

The most efficient electrode at optimum conditions is aluminum. The graph shows that aluminum generates approximately 46% and 42% more per minute with just about 12% and 7% additional power compared to stainless steel and DSA, respectively. As for the cost, microbubble generation using aluminum electrode is much cheaper by around 32 ~ 33% compared to using stainless steel and DSA (Fig. 7(b)). We have to note however that aluminum is a soluble electrode. So, in application, a more frequent replacement might be needed when using this type of electrode material.

Table 1. Operational cost summary of each electrode at different NaCl concentration

Electrode materials	Operational cost	NaCl concentration (g/L)								
		0.1	0.3	0.5	0.9	1.5	3	5	7	10
Aluminum	NaCl[a]	0.14	0.42	0.68	1.19	1.97	3.65	6.01	8.32	11.76
	Power[b]	1.72	0.70	0.45	0.26	0.19	0.11	0.08	0.06	0.05
	Total	**1.86**	**1.12**	**1.13**	**1.45**	**2.16**	**3.76**	**6.09**	**8.38**	**11.81**
Iron	NaCl[a]	0.32	0.97	1.64	3.03	5.08	9.87	16.16	23.15	32.77
	Power[b]	2.96	1.52	1.06	0.69	0.47	0.32	0.23	0.21	0.18
	Total	**3.28**	**2.49**	**2.70**	**3.72**	**5.55**	**10.19**	**16.39**	**23.36**	**32.95**
Stainless steel	NaCl[a]	0.25	0.73	1.22	2.21	3.66	7.05	12.93	19.06	28.74
	Power[b]	1.64	1.11	0.90	0.65	0.52	0.39	0.40	0.38	0.37
	Total	**1.89**	**1.84**	**2.12**	**2.86**	**4.18**	**7.44**	**13.33**	**19.44**	**29.11**
DSA	NaCl[a]	0.24	0.73	1.24	2.34	3.66	8.39	14.78	23.36	31.35
	Power[b]	2.14	0.97	0.75	0.59	0.45	0.40	0.36	0.38	0.34
	Total	**2.38**	**1.70**	**1.99**	**2.93**	**4.11**	**8.79**	**15.14**	**23.74**	**31.69**

a. Cost of NaCl (g) in every 1000 liters of microbubbles generated (USD)
b. Cost of power (kWh) in every 1000 liters of microbubbles generated (USD)

4. Conclusions

In this study, optimization of parameters in order to reduce operational cost of microbubble generation has been carried out using one-parameter-at-a-time approach. Based on the results, the parameter that has a direct relationship with the rate of microbubble generation is current density. Increasing the applied current into the system increases the rate of electrolysis and resulted to the increase in microbubble generation. The effect of NaCl on the rate of microbubble generation clearly depends on the electrode type and not on the amount. Addition of NaCl to a certain extent and narrowing the distance between electrodes had no significant changes on the rate of generation but tremendously decreased the power requirement of the process which reduced the operational cost of microbubble generation. Furthermore, comparison among four electrodes operating at optimum conditions revealed that aluminum is the most efficient electrode in terms of generation rate and cost outperforming the rest by a wide margin. However, we have to note that aluminum and iron are soluble electrodes. So in application, more frequent replacement is expected when using these electrodes during electrolysis.

REFERENCES

Adhoum, N., Monser, L., Bellakhal, N., Belgaied, J., 2004, Treatment of electroplating wastewater containing Cu^{2+}, Zn^{2+} and Cr(IV) by electrocoagulation, J. Hazard. Mater., B112, 207-213.

Alam, R., 2015, Fundamentals of electro-flotation and electrophoresis and applications in oil sand tailings management, Doctoral Dissertation, University of Western Ontario, Ontario, Canada.

Araya-Farias, M., Mondor, M., Lamarche, F., Tajchakavit, S., Makhlouf, J., 2008, Clarification of apple juice by electroflotation, Innov. Food Sci. Emerg., 9, 320-327.

Baierle, F., John, D. K., Souza, M. P., Bjerk, T. R., Moraes, M. S. A., Hoeltz, M., Rohlfes, A. L. B., Camargo, M. E., Corbellini, V. A., Schneider, R. C. S., 2015, Biomass from microalgae separation by electroflotation with iron and aluminum spiral electrodes, Chem. Eng. J., 267, 274-281.

Bande, R. M., Prasad, B., Mishra, I. M., Wasewar, K. L., 2008, Oil field effluent water treatment for safe disposal by electroflotation, Chem. Eng. J., 137, 503-509.

Bennet, A. J. R., Champmen, W. R., Dell, C. C., 1958, Studies in the froth flotation of coal, Third International Coal Preparation Congress, Brussels -Leige, E2, 452-462.

Bloom, F., Heindel, T. J., 2003, Modeling flotation separation in a semi-batch process, Chem. Eng. Sci., 58, 353-365.

Burns, S. E., Yiacoumi, S., Tsouris, C., 1997, Microbubble generation for environmental and industrial separations, Sep. Purif. Technol., 11, 221-232.

Casillas, H. A. M., Cocke, D. L., Gomes, J. A. G., Morkovsky, P., Parga, J. R., Peterson, E., Garcia, C., 2007, Electrochemistry behind electrocoagulation using iron electrode, The Electrochem. Soc. ECS Transact., 6, 1-15.

Chandran, P., Bakshi, S., Chatterjee, D., 2015, Study on the characteristics of hydrogen bubble formation and its transport during electrolysis of water, Chem. Eng. Sci., 138, 99-109.

Chen, G., 2004, Electrochemical technologies in wastewater treatment, Sep. Purif. Technol., 38, 11-41.

Chen, X., Chen, G., 2010, Electro-flotation in Comninellis, C., Chen, G. (eds.), Electrochemistry for the environment, Springer Science+Business Media, LLC., 263-277.

Gao, S., Yang, J., Tian, J., Ma, F., Tu, G., Du, M., 2010, Electro-coagulation-flotation process for algae removal, J. Hazard. Mater., 177, 336-343.

Goor, C., van de., 2015, Influence of temperature and pH on the Hydrogen Evolution Reaction (HER) on platinum, Undergraduate Thesis, University of Twente, Enschede, Netherlands.

Janssen, J. J. L., Sillen, C. W. M. P., Barendrecht, E., Van Stralen, S. J. D., 1984, Bubble behavior during oxygen and hydrogen evolution at transparent electrodes in KOH solution, Electrochim. Acta, 29, 633-642.

Ketlar, D. R., Mallikarjunan, R., Venkatachalam, S., 1991,

Electroflotation of quartz fine, Int. J. Miner. Process., 31, 127-138.

Keshmirizadeh, E., Yousefi, S., Rofouei, M. K., 2011, An Investigation on the new operational parameter effective in Cr(VI) removal efficiency: A Study on electrocoagulation by alternating pulse current, J. Hazard. Mater., 190, 119-124.

Khosla, N. K., Venkatachalam, S., 1991, Pulsed electrogeneration of bubbles for electroflotation, J. Appl. Electrochem., 21, 986-990.

Lee, J. E., Lee, J. K., 2002, Effect of microbubbles and particle size on the particle collection in the column flotation, Korean J. Chem. Eng., 19, 703-710.

Li, P., 2006, Development of advanced water treatment technology using microbubbles, Ph. D. Dissertation, Keio University, Tokyo, Japan.

Li, P., Tsuge, H., 2006, Water treatment by induced air flotation using microbubbles, J. Chem. Eng. Jpn., 39, 896-903.

Liuyi, R., Yimin, Z., Wenqing, Q., Shenxu, B., Peipei, W., Congren, Y., 2014, Investigation of condition-induced bubble size and distribution in electroflotation using a high-speed camera, Int. J. Min. Sci. Technol., 24, 7-12.

Mansour, L. B., Chalbi, S., Kesentini, I., 2007, Experimental study of hydrodynamic and bubble size distributions in electroflotation process, Indian J. Chem. Technol., 14, 253-257.

Mota, I. O., de Castro, J. A., Casqueira, R. G., de Oliveira, A. G., 2014, Study of electroflotation method for treatment of wastewater from washing soil contaminated by heavy metals, J. Mater. Res. Technol., 4, 109-113.

Nagai, N., Takeuchi, M., Kimura, T., Oka, T., 2003, Existence of optimum space between electrodes on hydrogen production by water electrolysis, Int. J. Hydrogen Ene., 28, 35-41.

Opu, M. S., 2015, Effect of operating parameters on performance of alkaline water electrolysis, Int. J. Thermal & Environ. Eng., 9, 53-60.

Park, Y. S., Kim, D. S., 2007, Study on bubble generation and size by dimensionally stable anode in electroflotation process, J. Environ. Sci. Int., 16(10), 1189-1195.

Parmar, R., Majumder, S. K., 2013, Microbubble generation and microbubble-aided transport process intensification-A State of the art report, Chem. Eng. Process., 64, 79-97.

Petrovic, J., Thomas, G., 2008, Reaction of aluminum with water to produce hydrogen, a study of issues related to the use of Aluminum for on-board vehicular hydrogen storage, U.S. Department of Energy.

Rahmani, A. R., Nematollahi, D., Godini, K., Azarian, G., 2013, Continuous thickening of activated sludge by electro-flotation, Sep. Purif. Technol., 107, 166-171.

Rubio, J., Souza, M. L., Smith, R. W., 2002, Overview of flotation as a wastewater treatment technique, Miner. Eng., 15, 139-155.

Tan, Y. J. K., Pham, B., Zong, Y., Perez, C., Maris, D. O., Hemphill, A., Miao, C. H., Matula, T. J., Mourad, P. D., Wei, H., Sellers, D., Horner, P. J., Pun, S. H., 2016, Microbubbles and ultrasound increase intraventricular polyplex gene transfer to the brain, J. Cont. Rel., 231, 86-93.

Weber, J., Agblevor, F. A., 2005, Microbubble fermentation of Trichoderma Reesei for cellulose production, Process. Biochem., 40, 669-676.